Biomimetic glycopolymers tethered gold nanoparticles: Preparation, self-assembly and lectin recognition properties

ARTICLE *in* COLLOIDS AND SURFACES B: BIOINTERFACES · DECEMBER 2014

Impact Factor: 4.15 · DOI: 10.1016/j.colsurfb.2014.11.046

6 AUTHORS, INCLUDING:

Qingrong Huang
Rutgers, The State University of New Jersey
118 PUBLICATIONS **2,163** CITATIONS
SEE PROFILE

Fan Li
changchun institue of applied chemistry,C…
12 PUBLICATIONS **140** CITATIONS
SEE PROFILE

Tongfei Shi
Chinese Academy of Sciences
85 PUBLICATIONS **634** CITATIONS
SEE PROFILE

Colloids and Surfaces B: Biointerfaces 126 (2015) 367–373

Contents lists available at ScienceDirect

Colloids and Surfaces B: Biointerfaces

journal homepage: www.elsevier.com/locate/colsurfb

Biomimetic glycopolymers tethered gold nanoparticles: Preparation, self-assembly and lectin recognition properties

Danfeng Pei[a], Yanchun Li[b], Qingrong Huang[c], Qu Ren[d], Fan Li[a,*], Tongfei Shi[a,*]

[a] State Key Laboratory of Polymer Physics and Chemistry, Changchun Institute of Applied Chemistry, Chinese Academy of Sciences, Changchun 130022, PR China
[b] Department of Pediatric Respiratory Medicine, First Hospital of Jilin University, Jilin Province 130021, PR China
[c] Food Science Department, Cook College, Rutgers University, New Brunswick, NJ 08901-8520,United States
[d] Clinical Laboratory Center, Air Force General Hospital, No. 30 Fucheng Road, Haidian District, Beijing 100142, PR China

ARTICLE INFO

Article history:
Received 23 June 2014
Received in revised form
25 November 2014
Accepted 30 November 2014
Available online 8 December 2014

Keywords:
Glycopolymer
Degradable
Gold nanoparticle
Self-assembly
Lectin recognition

ABSTRACT

Biomimetic glycopolymers poly(gluconamidoethylmethacrylate)-b-poly(ε-caprolactone)-b-poly(gluconamidoethylmethacrylate) with degradable disulfide groups in the backbone (PGAMA-PCL-SS-PCL-PGAMA) were synthesized by the combination of ring opening polymerization (ROP) and atom transfer radical polymerization (ATRP). The internal disulfide bonds were cleaved by reduction with DL-dithiothreitol to yield the corresponding thiol terminated glycopolymers. The thiol terminated glycopolymers were effectively anchored on the surface of gold nanoparticles to prepare the biomimetic glycopolymers modified gold nanoparticles (Gly@Au NPs). Moreover, the properties of the Gly@Au NPs in aqueous solution were investigated. Transmission electron microscopy (TEM) analysis revealed that the self-assembly morphology of the Gly@Au NPs can be fine-tuned, from irregular clusters to spherical aggregates, by changing the weight fraction of the hydrophobic PCL block. Furthermore, the Gly@Au NPs had specific recognition with Concanavalin A (Con A).

1. Introduction

Recently, hybrid nanoparticles composed of an inorganic core and an organic polymer shell have received considerable attention as a new class of nanoscale materials [1–5]. The hybrid nanoparticles have held a significant promise in the areas of sensing, catalysis, and biomedical applications [6–12]. Gold nanoparticles (Au NPs), owing to their ease of synthesis, functionalization and extensively biological applications have attracted particular interest [13–16]. For biological applications, in order to target them to specific disease areas or allow them to selectively interact with cells, biological modification is essential. The carbohydrate polymers, referred to as glycopolymers, are known to have specific interaction with lectins [17–19]. Thus, the glycopolymers modified Au NPs could be served as potential nanomaterials for sensing and targeted biological applications [20–24].

Au NPs functionalized with amphiphilic glycopolymers would be more interesting. A few articles have reported that the block polymers such as PEO-b-PS and PEO-b-PB tethered Au NPs could self-assemble into various morphology [25–27]. Thus, the modified amphiphilic glycopolymers may induce the hybrid nanoparticles to self-assemble into well-defined nanostructures such as micelles and vesicles with carbohydrate containing shell in aqueous solution. Furthermore, in some cases, the self-assembled hybrid nanoparticles coupled the electronic and optical properties of individual nanoparticles in their clusters, leading to new, interesting and potentially useful properties of the ensembles [28,29]. Therefore, the self-assembled Gly@Au NPs nanostructures may be served as catalytic reactors for chemical synthesis or targeted delivery vehicles for drugs with enhanced contrast imaging. Although the Gly@Au NPs may have broad applications in glycobiology or photothermal therapy, the research on the Gly@Au NPs are still rare.

Here, we described the preparation of the Gly@Au NPs. The glycopolymers with thiol end groups were effectively anchored on the surface of gold nanoparticles using the ligand exchange method. The thiol terminated glycopolymers were produced by the reduction of the disulfide containing amphiphilic glycopolymers, which were synthesized by the combination of ROP and ATRP. The self-assembly properties of the Gly@Au NPs were investigated using UV–vis spectroscopy, dynamic light scattering (DLS) and TEM. The self-assembly morphology of Gly@Au NPs evolved from irregular clusters to spherical aggregates with the increasing weight fraction

* Corresponding authors. Tel.: +86 431 85262137.
E-mail addresses: fli1216@ciac.ac.cn (F. Li), tfshi@ciac.ac.cn (T. Shi).

http://dx.doi.org/10.1016/j.colsurfb.2014.11.046
0927-7765/

of the hydrophobic PCL block. Furthermore, the lectin recognition properties of the Gly@Au NPs with Con A were studied by means of UV–vis spectroscopy, DLS and TEM, which demonstrated that the Gly@Au NPs had specific recognition with Con A.

2. Experimental

2.1. Materials

Stannous octoate, bis(2-hydroxyethyl) disulfide, 2-bromo-2-methylpropionic acid, D-gluconolactone, dicyclohexylcarbodiimide (DCC), *N*,*N*-dimethylamino pyridine (DMAP), 2-aminoethyl methacrylate hydrochloride, DL-dithiothreitol (DTT), bipyridine, N-methyl-2-pyrrolidone (NMP), sodium citrate, hydrogen tetrachloroaurate(III) hydrate were all purchased from Sigma–Aldrich and used as received. ε-Caprolactone (Sigma–Aldrich), toluene (Beijing Chemical Reagent Co., Ltd.), dichloromethane (DCM) (Beijing Chemical Reagent Co., Ltd.) were distilled from CaH_2, respectively. Copper(I) bromide (98%, Sigma–Aldrich) was purified by a washing with glacial acetic acid followed by methanol. D-Gluconamidoethyl methacrylate (GAMA) glycomonomer was synthesized from D-gluconolactone and 2-aminoethyl methacrylate hydrochloride according to the literature procedure (70.0% yield) [30]. Gold nanoparticles (Au NPs) were prepared by sodium citrate and hydrogen tetrachloroaurate(III) hydrate according to the literature [31] (the particle size was 18.64 ± 1.78 nm determined by TEM).

2.2. Methods

Molecular weight and molecular weight distribution (M_w/M_n) of polymers were determined on a gel permeation chromatograph (GPC, PL-GPC 50 Plus, Varian) with DMF containing 0.01 M LiBr as eluent (flow rate: 1 mL/min, at 50 °C) against poly(methyl methacrylate) standards. ^{1}H NMR spectra were recorded at room temperature on a Bruker AV 400 MHz spectrometer. $CDCl_3$, DMSO-d_6 were used as the deuterated solvents. UV–vis spectra were recorded at room temperature using a TU-1901 UV–vis spectrophotometer. The mean size of nanoparticles was determined by DLS using a Malvern Nano ZS instrument (scattering angle: 173° and at 25 °C). TEM was performed using a JEM 1011 at a 100 kV accelerating voltage.

2.3. Synthesis of degradable disulfide containing biomimetic glycopolymers by the combination of ROP and ATRP

Degradable disulfide containing biomimetic glycopolymers PGAMA-PCL-SS-PCL-PGAMA were synthesized as shown in Scheme 1. Firstly, poly(ε-caprolactone) with an internal disulfide bond and two hydroxyl end groups (HO-PCL-SS-PCL-OH) was synthesized by the controlled ROP of ε-caprolactone monomer using bis(2-hydroxyethyl) disulfide as an initiator and stannous octoate as a catalyst at 110 °C for 24 h. After cooling to room temperature, the crude product was dissolved in DCM and precipitated into cold methanol to give white solid, which was dried in vacuum to constant weight in a yield of 95.0%. ^{1}H NMR ($CDCl_3$, δ ppm) of HO-PCL_{69}-SS-PCL_{69}-OH sample: 1.38 (m, 276H, —$COCH_2CH_2C\mathbf{H_2}CH_2CH_2O$—), 1.63 (m, 552H, —$COCH_2C\mathbf{H_2}CH_2C\mathbf{H_2}CH_2O$—), 2.28 (m, 276H, —$COC\mathbf{H_2}CH_2CH_2CH_2CH_2O$—), 3.65 (t, 4H,—$C\mathbf{H_2}OH$), 4.05(m, 276H, —$COCH_2CH_2CH_2CH_2C\mathbf{H_2}O$—).

Then HO-PCL-SS-PCL-OH was converted into ATRP macroinitiator Br-PCL-SS-PCL-Br via esterification with 2-bromo-2-methylpropionic acid. A typical example was given below. HO-PCL_{69}-SS-PCL_{69}-OH precursor (1.50 g, 0.1 mmol) was dissolved in dry DCM (3 mL). The flask containing the solution was then immersed in ice-water bath, and 2-bromo-2-methylpropionic acid (50.10 mg, 0.3 mmol) was added upon stirring, followed by a solution of DCC (61.90 mg, 0.3 mmol) in 1 mL of DCM. The mixture was then stirred for 10 min in the cooling bath, and a solution of DMAP (36.65 mg, 0.3 mmol) in 2 mL of DCM was added dropwise. The resulting heterogeneous mixture was stirred at room temperature for 60 h. Dicyclohexylurea was removed by filtration, the filtrate was concentrated and precipitated under vigorous stirring into 50 mL methanol. The solid was filtered and dried under reduced pressure (92.0% yield). ^{1}H NMR ($CDCl_3$, δ ppm) of Br-PCL_{69}-SS-PCL_{69}-Br sample: 1.38 (m, 276H, —$COCH_2CH_2C\mathbf{H_2}CH_2CH_2O$), 1.63 (m, 552H, —$COCH_2C\mathbf{H_2}CH_2C\mathbf{H_2}CH_2O$—), 1.86 (s, 12H, —$C(C\mathbf{H_3})_2$—), 2.28 (m, 276H, —$COC\mathbf{H_2}CH_2CH_2CH_2CH_2O$—), 4.05 (m, 276H, —$COCH_2CH_2CH_2CH_2C\mathbf{H_2}O$—).

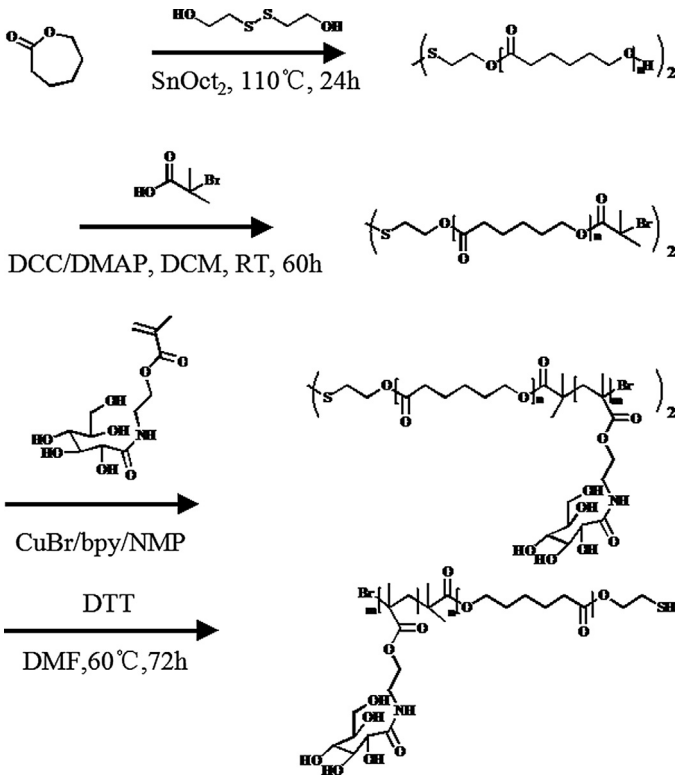

Scheme 1. Synthesis of degradable disulfide containing biomimetic glycopolymer PGAMA-PCL-SS-PCL-PGAMA and its reduction to form thiol terminated biomimetic glycopolymer PGAMA-PCL-SH.

Finally, PGAMA-PCL-SS-PCL-PGAMA was synthesized by the ATRP of GAMA using Br-PCL-SS-PCL-Br as macroinitiator [32]. Typically, Br-PCL_{69}-SS-PCL_{69}-Br macroinitiator (1.5 g, 0.1 mmol) and GAMA glycomonomer (1.29 g, 4 mmol) were dissolved in NMP (4 mL) at room temperature and the mixture solution was degassed via nitrogen purge for 30 min. Copper(I) bromide (28.69 mg, 0.2 mmol) and bipyridine (62.48 mg, 0.4 mmol) were added in turn, and the resulting solution was degassed again for 10 min and then stirred vigorously under nitrogen at room temperature for 24 h. The mixture was precipitated into isopropanol (20 mL), and washed sequentially by THF (2 mL) and heated methanol (5 mL) and then dried under reduced pressure. The yield was 69.4%. ^{1}H NMR (DMSO-d_6, δ ppm) of $PGAMA_{17}$-PCL_{69}-SS-PCL_{69}-$PGAMA_{17}$ sample: 0.6–1.0 (m, 102H, —$C(C\mathbf{H_3})$—), 1.6–2.0(m, 68H, —$C(C\mathbf{H_2})$—), 1.30 (m, 276H, —$COCH_2CH_2C\mathbf{H_2}CH_2CH_2O$), 1.54 (m, 552H, —$COCH_2C\mathbf{H_2}CH_2C\mathbf{H_2}CH_2O$—), 1.86 (s, 12H, —$C(C\mathbf{H_3})_2$—), 2.28 (m, 276H, —$COC\mathbf{H_2}CH_2CH_2CH_2CH_2O$—), 3.98 (m, 276H, —$COCH_2CH_2CH_2CH_2C\mathbf{H_2}O$—), 3.38–3.66 and 4.02–4.63 (glucose residue).

Table 1
Characterization of degradable disulfide containing biomimetic glycopolymers PGAMA-PCL-SS-PCL-PGAMA.

	Composition[a]	M_n		PDI
		GPC[b]	NMR[c]	
1	$(PGMA_{14}\text{-}PCL_{32}\text{-}S)_2$	18,430	15,540	1.25
2	$(PGMA_{17}\text{-}PCL_{69}\text{-}S)_2$	36,090	25,200	1.27
3	$(PGMA_{15}\text{-}PCL_{240}\text{-}S)_2$	117,560	59,450	1.20

[a] The subscript numbers represent the repeating units number of each block determined by ^{1}H NMR.
[b] Number average molecular weight determined by GPC using poly(methyl methacrylate) standards for calibration.
[c] Molecular weight calculated from ^{1}H NMR measurements.

2.4. Reduction of the disulfide containing biomimetic glycopolymers

The reduction of the internal disulfide bonds of PGAMA-PCL-SS-PCL-PGAMA were shown in Scheme 1. The internal disulfide bonds were cleaved by reduction with DL-dithiothreitol to yield the corresponding thiol terminated glycopolymers [33]. In a typical procedure, $PGAMA_{17}\text{-}PCL_{69}\text{-}SS\text{-}PCL_{69}\text{-}PGAMA_{17}$ (2.50 g, 0.1 mmol) was dissolved in 6 mL of deoxygenated DMF. Then, DTT (1.54 g, 10 mmol) was added. The mixtures were stirred under nitrogen at 60 °C for 72 h. The final product was precipitated into methanol and then dried under reduced pressure.

2.5. Surface modification of the AuNPs

Thiol ended PGAMA-PCL-SH (10 mg) was first dissolved in 10 mL of DMF. Then, a concentrated solution of Au NPs (~2 mg/mL) was slowly added to the above solution under vigorous shaking. Subsequently, the mixture was sonicated for 30 min to avoid the aggregates of Au NPs. The solution was then steadily kept for overnight to finish the ligand exchange. The glycopolymer modified Au NPs were further purified by centrifuged (8000 rpm, 30 min) for 6 times and redispersed in DMF at a concentration of 1 mg/mL.

2.6. The self-assembly and recognition properties of the Gly@Au NPs

The gold nanoparticles stabilized with PGAMA-PCL-SH were dissolved in DMF (1 mg/mL), and distilled water (30 wt%) was then added gradually. After stirring for 24 h at room temperature, DMF was removed by dialyzing (MWCO = 6000) against distilled water for 2 days. Then, the concentration was adjusted to 0.5 mg/mL.

The self-assembly properties of the Gly@Au NPs and the recognition with Con A were investigated in aqueous solution at room temperature and measured by UV–vis spectroscopy, DLS and TEM.

3. Results and discussion

3.1. Synthesis of degradable disulfide containing biomimetic glycopolymers by the combination of ROP and ATRP

ATRP technique has been proved to be a robust strategy for the synthesis of well-defined glycopolymers with unprotected glycomonomers [30,32]. The glycopolymers PGAMA-PCL-SS-PCL-PGAMA were synthesized as shown in Scheme 1. Three samples containing the similar length of hydrophilic segment (PGAMA) but different length of hydrophobic segment (PCL) were obtained (Table 1). The chain structures and chemical compositions of the amphiphilic glycopolymers were characterized by ^{1}H NMR (Fig. 1) and GPC (Fig. 2A), respectively. It can be seen from Fig. 1B that the proton signals of the HO-PCL-SS-PCL-OH precursor (Fig. 1A) at 3.65 ppm assignable to the primary hydroxyl methylene end

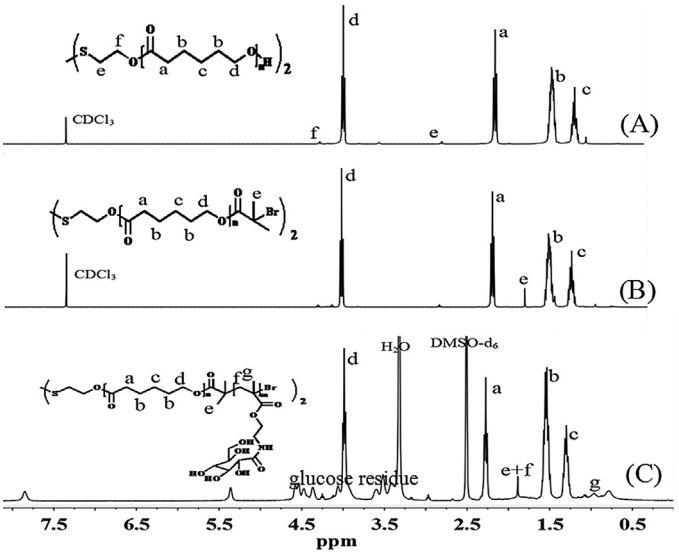

Fig. 1. ^{1}H NMR spectra of HO-PCL-SS-PCL-OH in $CDCl_3$ (A), Br-PCL-SS-PCL-Br in $CDCl_3$ (B) and PGAMA-PCL-SS-PCL-PGAMA in DMSO-d_6 (C).

group (HOC**H$_2$**—) disappeared. Simultaneously, the characteristic peaks of 2-bromo-2-methylpropionic acid segments of Br-PCL-SS-PCL-Br appeared at 1.86 ppm assignable to the proton signals of methyl (—C(C**H$_3$**)$_2$—). Moreover, the integral ratio of the proton signal on 2-bromo-2-methylpropionic acid end group to the repeating methylene unit of Br-PCL-SS-PCL-Br was very close to the theoretical value. These results showed that the hydroxyl end groups of HO-PCL-SS-PCL-OH precursor were quantitatively converted into 2-bromo-2-methylpropionic acid end groups within Br-PCL-SS-PCL-Br. Fig. 1C showed the ^{1}H NMR of the products PGAMA-PCL-SS-PCL-PGAMA. New characteristic proton signals concerning to PGAMA segment appeared at 0.6–1.0, 1.6–2.0 and 2.8–4.7 ppm, which were assigned to methyl protons (—C(C**H$_3$**)—), methylene protons (—C(C**H$_2$**)—) and glucose residue protons of PGAMA block, respectively. The integral ratio of the proton signal on PGAMA repeating methyl protons (—C(C**H$_3$**)—) to the repeating methylene on PCL was used to calculate the number of the GAMA unit. The molecular weight and molecular weight distribution were shown in Fig. 2A. The GPC curves showed symmetrical and unimodal elution peaks and no shoulder peaks or tailing were observed, denoting well-defined biomimetic glycopolymers. The retention time of $PGAMA_{15}\text{-}PCL_{240}\text{-}SS\text{-}PCL_{240}\text{-}PGAMA_{15}$ (Fig. 2A) was 11.0 min which was slightly shorter than that of $Br\text{-}PCL_{240}\text{-}SS\text{-}PCL_{240}\text{-}Br$ (11.4 min). The M_n of $Br\text{-}PCL_{240}\text{-}SS\text{-}PCL_{240}\text{-}Br$ and $PGAMA_{15}\text{-}PCL_{240}\text{-}SS\text{-}PCL_{240}\text{-}PGAMA_{15}$ calculated from GPC were 97,700 and 117,500 g/mol, respectively. These results indicated the successful chain extension of the macroinitiator. The PDI calculated from the GPC was roughly narrow (Table 1).

3.2. Reduction of the disulfide containing biomimetic glycopolymers

The products PGAMA-PCL-SS-PCL-PGAMA containing internal disulfide bonds should be reduced to form thiol terminated glycopolymers for the following study. A variety of reagents have been used for the reduction [33,34]. DTT, a kind of reducing agent, due to its low redox potential, mild reaction conditions and solubility in a range of solvent, was selected for the purposes of this study.

Reduction of the PGAMA-PCL-SS-PCL-PGAMA molecules were performed in DMF solvent at 60 °C. The oxygen free condition was required among the whole reaction process. The degree of reduction can be conveniently followed by GPC. The disulfide bonds

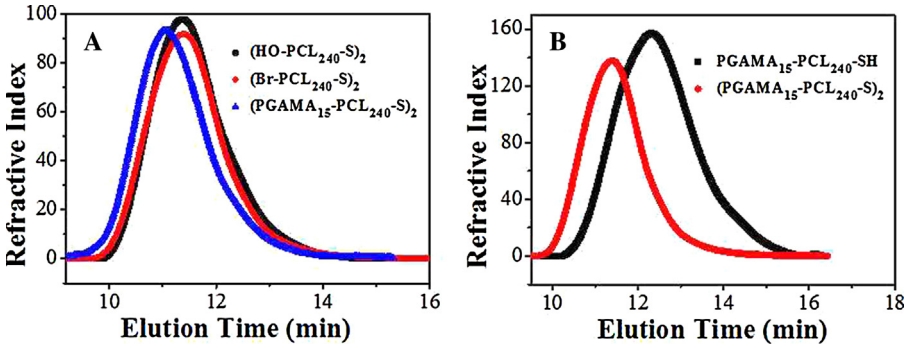

Fig. 2. GPC traces of disulfide containing polymers HO-PCL-SS-PCL-OH, Br-PCL-SS-PCL-Br, PGAMA-PCL-SS-PCL-PGAMA (A) and the reduced products PGMA-PCL-SH (B).

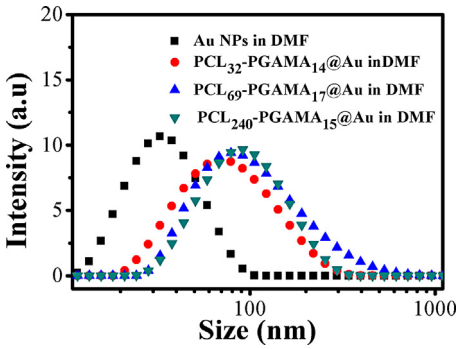

Fig. 3. Particle size of Au NPs and PCL-PGAMA@Au in DMF determined by DLS.

were completely reduced to thiol groups after 72 h. Fig. 2B showed the changes of the GPC traces. The molecular weight of $PGAMA_{15}$-PCL_{240}-SH calculated from the GPC traces was 45,140 g/mol almost half of the $PGAMA_{15}$-PCL_{240}-SS-PCL_{240}-$PGAMA_{15}$ and the unimodal trace indicated the total reduction.

The successful reduction of PGAMA-PCL-SS-PCL-PGAMA to thiol terminated glycopolymers PGAMA-PCL-SH was also confirmed by ^{1}H NMR (Fig. S1(A)) and FT-IR (Fig. S1(B)). It can be seen from Fig. S1(A) that the proton signal at 1.43 ppm assignable to the thiol group appeared. Moreover, the integral ratio of the proton signal on thiol end group to the repeating methylene unit of $PGAMA_{17}$-PCL_{69}-SH was very close to the theoretical value. The FT-IR spectra of the $PGAMA_{17}$-PCL_{69}-SH glycopolymer (Fig. S1(B)) showed a tiny band at 2570 cm^{-1}, which was assigned to the stretching vibration of thiol groups.

3.3. Preparation of the biomimetic glycopolymers tethered gold nanoparticles

Thiol groups exhibit strongly binding ability with Au NPs. Thus, the thiol terminated glycopolymers PGAMA-PCL-SH can be used to modify the Au NPs using the ligand exchange method. The formed Gly@Au NPs dispersed in DMF were characterized by DLS and TEM. The DLS curves (Fig. 3) showed symmetrical and unimodal peaks. The particles size increased after modification. The size of the original Au NPs was about 30 nm determined by DLS. As the length of the PCL block increasing, the size increased (64 nm for PCL_{32}-$PGAMA_{14}$@Au NPs, then 80 nm for PCL_{69}-$PGAMA_{17}$@Au NPs and 90 nm for PCL_{240}-$PGAMA_{15}$@Au NPs in DMF). Then, TEM was used to observe the morphology of the Gly@Au NPs (Fig. S2). The TEM results indicated that all the Gly@Au NPs could disperse in DMF individually. The obtained Gly@Au NPs dispersed in DMF could be stored at ambient conditions over several weeks. These results indicated that the Gly@Au NPs were prepared successfully and can disperse in DMF stably.

3.4. Self-assembly properties of the Gly@Au NPs

Like the amphiphilic polymers, the self-assembly properties of the Gly@Au NPs were also controlled by the hydrophobic interactions, which were influenced by weight fraction of the hydrophobic PCL block. The self-assembly properties of the Gly@Au NPs were investigated in aqueous solution by means of UV–vis spectroscopy, DLS and TEM. Fig. 4A shows the UV–vis spectra of the Gly@Au NPs. The spectra revealed a red-shifted absorbance band in the range investigated as the length of the PCL block increasing. For PCL_{32}-$PGAMA_{14}$@Au NPs, the maximum of the localized surface plasmon resonance (LSPR) band was 520 nm, which was the same as the original Au NPs. The result indicated that no aggregates were formed when PCL_{32}-$PGAMA_{14}$@Au NPs dispersed in aqueous solution [35]. The maximum of the LSPR band shifted to 530 nm and 548 nm for PCL_{69}-$PGAMA_{17}$@Au NPs and PCL_{240}-$PGAMA_{15}$@Au NPs, respectively. Moreover, the LSPR band was broadened as the length of the PCL block increasing. The UV–vis spectra results indicated that as the length of the PCL block increasing, the interparticle distances

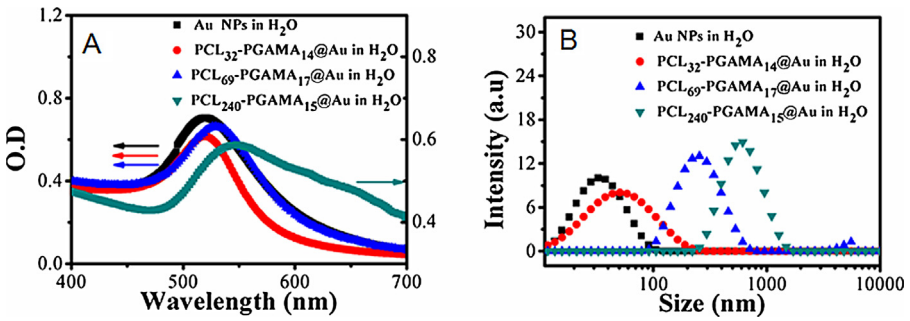

Fig. 4. UV–vis spectra of the self-assembled PCL-PGAMA@Au with increasing weight fraction of the hydrophobic PCL block (A) and the particle size of Au NPs and PCL-PGAMA@Au in H_2O determined by DLS (B).

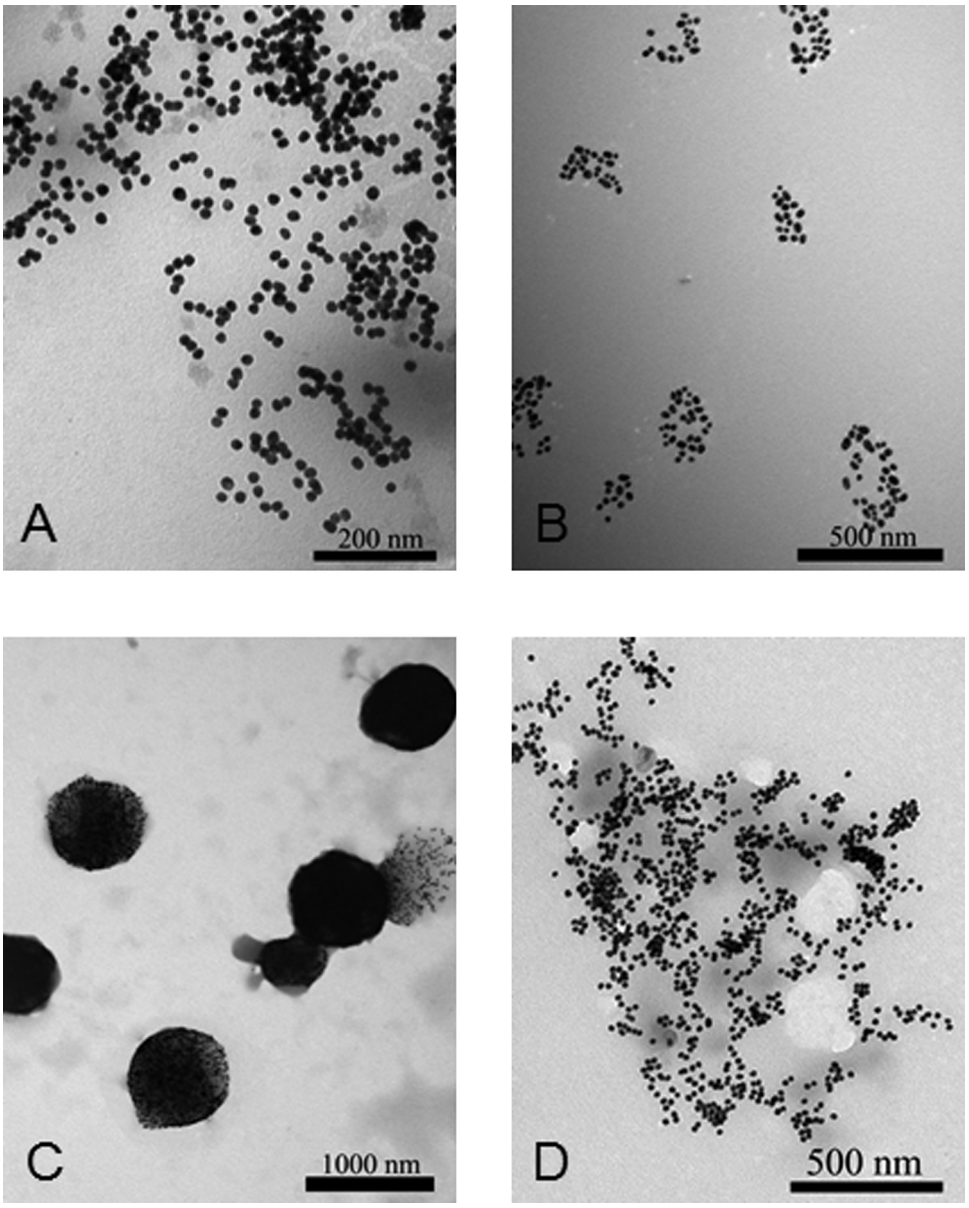

Fig. 5. TEM photographs of (A) PCL_{32}-$GAMA_{14}$@Au, (B) PCL_{69}-$GAMA_{17}$@Au, (C) PCL_{240}-$GAMA_{15}$@Au and (D) PCL_{32}-$GAMA_{14}$@Au@Con A in aqueous solution.

were progressive decrease and large clusters may form in the aqueous solution.

Furthermore, DLS was also used to study the self-assembly properties of the Gly@Au NPs (Fig. 4B). As the length of the PCL block increasing, the size increased from 50 nm to 580 nm. For PCL_{32}-$PGAMA_{14}$@Au NPs, the particle size was about 50 nm in aqueous solution, which was similar to that in DMF (64 nm) (the differences in size may be caused by the different solubility of the PCL_{32}-$PGAMA_{14}$ shell in aqueous solution and DMF). The DLS result also indicated that the PCL_{32}-$PGAMA_{14}$@Au NPs dispersed in aqueous solution individually. The size of PCL_{69}-$PGAMA_{17}$@Au NPs and PCL_{240}-$PGAMA_{15}$@Au NPs in aqueous solution was about 270 nm and 580 nm, while the size in DMF was only about 78 nm and 90 nm, respectively. The results meant that large clusters may form in the aqueous solution.

To verify these hypotheses, TEM was used to observe the Gly@Au NPs aggregates (Fig. 5). As expected, PCL_{32}-$PGAMA_{14}$@Au NPs (Fig. 5A) appeared as individual particles and absolutely no particles aggregates were observed. It is probably because the hydrophobic interactions were too weak to drive the individual particles to form the clusters. Thus the particles can disperse in water stably. Fig. 5B, PCL_{69}-$PGAMA_{17}$@Au NPs containing longer PCL block, showed the formation of the nanoparticle clusters, but regular shape was not formed. Interestingly, further increasing the PCL length, the Gly@Au NPs self-assembled into spherical aggregates (Fig. 5C). The size of the PCL_{240}-$PGAMA_{15}$@Au NPs in aqueous solution was about 789 ± 120 nm. These relatively broad size distribution was indeed typical for superparticles made from nanoparticle assembly. Moreover, the distance between the Gly@Au NPs decreased as the chain length increasing. This was due to the increasing hydrophobic interaction of interparticles as the increasing hydrophobic segment length, leading to a more compact structure. The self-assembly morphology of the Gly@Au NPs evolved from irregular clusters to spherical aggregates, and the distance between the Au NPs can be tuned by changing the PCL length. The results indicated that the hydrophobic interactions played a critical role in the Gly@Au NPs self-assembly.

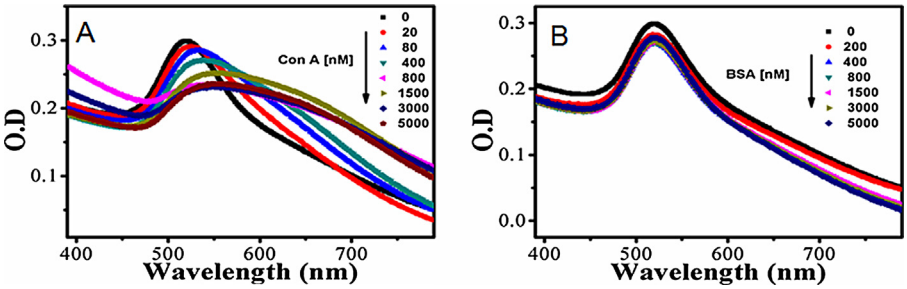

Fig. 6. UV–vis spectra of PCL_{32}-$PGAMA_{14}$@Au on addition of Con A (A) and BSA (B).

3.5. Recognition properties of the Gly@Au NPs

Carbohydrate can selectively bind protein. It is reported that Con A specifically recognizes D-glucopyranoside and D-mannopyranoside residues with free 3-, 4-, and 6-hydroxyl groups, and the binding of Con A with glycopolymers usually results in the Con A-cross-linked aggregates [36–38]. The interactions between Con A and the Gly@Au NPs were investigated in aqueous solution at room temperature.

UV–vis spectroscopy, DLS and TEM were employed to examine the specific recognition properties. In Fig. 6A as the concentration of Con A increasing, the UV–vis spectra showed a red shift of the maximum of LSPR band, from 520 nm to 555 nm, indicating the formation of the Con A-cross-linked aggregates. The UV–visible spectra showed the sensitive change, induced by addition of only 20 nM Con A. In order to determine the specific recognition properties, bovine serum albumin (BSA) was selected as a control [39]. The maximum of LSPR band did not shift with addition of the BSA protein (Fig. 6B). Moreover, DLS were also used to determine the specific recognition. In Fig. S3(A), as the concentration of Con A increasing the particle size increased. But the size did not change with addition of the noncorresponding protein BSA (Fig. S3(B)). The results confirmed that the Gly@Au NPs had specific recognition with Con A, which caused Gly@Au@Con A precipitates.

The specific recognition properties can be clarified by the following TEM analysis. In Fig. 5D, we can clearly see that the irregular clusters were formed between Con A and the Gly@Au NPs, and no individual Gly@Au NPs was observed in the complex solution. The results suggested that the binding between Gly@Au NPs and Con A occurred and resulted in the Con A-cross-linked aggregates. Aggregates were not observed by TEM on addition of BSA (Fig. S4(D)). In conclusion, the above analysis indicated that these Gly@Au NPs have specific binding with Con A in aqueous solution, which provides them useful for targeted delivery and therapeutics.

4. Conclusions

We prepared the biomimetic glycopolymers modified gold nanoparticles (Gly@Au NPs) and investigated their self-assembly and lectin recognition properties. The biomimetic glycopolymers with thiol end groups effectively anchored on the surface of gold nanoparticles using the ligand exchange method. The thiol terminated glycopolymers were produced by reducing the disulfide containing biomimetic glycopolymers PGAMA-PCL-SS-PCL-PGAMA, which were synthesized by the combination of ROP and ATRP. TEM, DLS and UV–vis spectroscopy were used to investigate the properties of the Gly@Au NPs in aqueous solution. The morphology of the self-assembled Gly@Au NPs evolved from irregular clusters to spherical aggregates, and the distance between the Gly@Au NPs can be tuned by changing the PCL length. Furthermore, the Gly@Au NPs can bind Con A effectively to form the stable ConA-cross-linked aggregates in aqueous solution. Consequently, the Gly@Au NPs may be used as potential nanomaterials for targeted biological applications such as delivery vehicles or photothermal therapy.

Acknowledgments

This work is supported by the National Natural Science Foundation of China (grant nos. 51028301494, 81100014 and 21174146). Programs and subsidized by the Special Funds for National Basic Research Program of China (grant no. 2009CB930100). We thank Prof. Zhihong Nie for a helpful discussion.

Appendix A. Supplementary data

Supplementary data associated with this article can be found, in the online version, at http://dx.doi.org/10.1016/j.colsurfb.2014.11.046.

References

[1] C. Rossner, B. Ebeling, P. Vana, ACS Macro Lett. 2 (2013) 1073–1076.
[2] D.D.B. Ouboter, T.B. Schuster, S.J. Sigg, W.P. Meier, Colloids Surf. B: Biointerfaces 112 (2013) 542–547.
[3] J.S. Basuki, L. Esser, H.T.T. Duong, Q. Zhang, P. Wilson, M.R. Whittaker, D.M. Haddleton, C. Boyer, T.P. Davis, Chem. Sci. 5 (2014) 715–726.
[4] M. Lattuada, T.A. Hatton, J. Am. Chem. Soc. 129 (2007) 12878–12889.
[5] T. Simon, S.C. Boca, S. Astilean, Colloids Surf. B: Biointerfaces 97 (2012) 77–83.
[6] A.B.R. Mayer, J.E. Mark, Colloid Polym. Sci. 275 (1997) 333–340.
[7] A. Pfaff, A. Schallon, T.M. Ruhland, A.P. Majewski, H. Schmalz, R. Freitag, A.H.E. Muller, Biomacromolecules 12 (2011) 3805–3811.
[8] H.P.O. Nascimento, M.D.L. Oliveira, C.P. de Melo, G.J.L. Silva, M.T. Cordeiro, C.A.S. Andrade, Colloids Surf. B: Biointerfaces 86 (2011) 414–419.
[9] M. Mathew, S. Sureshkumar, N. Sandhyarani, Colloids Surf. B: Biointerfaces 93 (2012) 143–147.
[10] N. Uehara, Anal. Sci. 26 (2010) 1219–1228.
[11] R. Ladj, A. Bitar, M.M. Eissa, H. Fessi, Y. Mugnier, R. Le Dantec, A. Elaissari, Int. J. Pharm. 458 (2013) 230–241.
[12] R. Francis, N. Joy, E.P. Aparna, R. Vijayan, Polym. Rev. 54 (2014) 268–347.
[13] A. Majzik, L. Fulop, E. Csapo, F. Bogar, T. Martinek, B. Penke, G. Biro, I. Dekany, Colloids Surf. B: Biointerfaces 81 (2010) 235–241.
[14] M. Shah, V.D. Badwaik, R. Dakshinamurthy, J. Nanosci. Nanotechnol. 14 (2014) 344–362.
[15] R.A. Sperling, P. Rivera gil, F. Zhang, M. Zanella, W.J. Parak, Chem. Soc. Rev. 37 (2008) 1896–1908.
[16] S.J. Guo, E.K. Wang, Anal. Chim. Acta 598 (2007) 181–192.
[17] C.R. Becer, Macromol. Rapid Commun. 33 (2012) 742–752.
[18] H. Kitano, Y. Takahashi, K. Mizukami, K. Matsuura, Colloids Surf. B: Biointerfaces 70 (2009) 91–97.
[19] K. Kobayashi, A. Tsuchida, T. Usui, T. Akaike, Macromolecules 30 (1997) 2016–2020.
[20] A. Housni, H.J. Cai, S.Y. Liu, S.H. Pun, R. Narain, Langmuir 23 (2007) 5056–5061.
[21] A.L. Parry, N.A. Clemson, J. Ellis, S.S.R. Bernhard, B.G. Davis, N.R. Cameron, J. Am. Chem. Soc. 135 (2013) 9362–9365.
[22] C.M. Dong, Comb. Chem. High Throughput Screen. 14 (2011) 173–181.
[23] M. Takara, M. Toyoshima, H. Seto, Y. Hoshino, Y. Miura, Polym. Chem. 5 (2014) 931–939.
[24] Z.C. Deng, S.Q. Li, X.Z. Jiang, R. Narain, Macromolecules 42 (2009) 6393–6405.
[25] A. Sanchez-Iglesias, M. Grzelczak, T. Altantzis, B. Goris, J. Perez-Juste, S. Bals, G. Van Tendeloo, S.H. Donaldson, B.F. Chmelka, J.N. Israelachvili, L.M. Liz-Marzan, ACS Nano 6 (2012) 11059–11065.
[26] J.B. Song, L. Cheng, A.P. Liu, J. Yin, M. Kuang, H.W. Duan, J. Am. Chem. Soc. 133 (2011) 10760–10763.
[27] J. He, Y.J. Liu, T. Babu, Z.J. Wei, Z.H. Nie, J. Am. Chem. Soc. 134 (2012) 11342–11345.

[28] A. Lee, A. Ahmed, D.P. dos Santos, N. Coombs, J.I. Park, R. Gordon, A.G. Brolo, E. Kumacheva, J. Phys. Chem. C 116 (2012) 5538–5545.
[29] T. Toyota, N. Ohguri, K. Maruyama, M. Fujinami, T. Saga, I. Aoki, Anal. Chem. 84 (2012) 3952–3957.
[30] R. Narain, S.P. Armes, Biomacromolecules 4 (2003) 1746–1758.
[31] G. Frens, Nat. Phys. Sci. 241 (1973) 20–22.
[32] X.H. Dai, C.M. Dong, J. Polym. Sci. A: Polym. Chem. 46 (2008) 817–829.
[33] N.V. Tsarevsky, K. Matyjaszewski, Macromolecules 35 (2002) 9009–9014.
[34] P.C. Jocelyn, Methods Enzymol. 143 (1987) 246–256.
[35] M.D. Zhu, L.Q. Wang, G.J. Exarhos, A.D.Q. Li, J. Am. Chem. Soc. 126 (2004) 2656–2657.
[36] C.R. Bertozzi, L.L. Kiessling, Science 291 (2001) 2357–2364.
[37] C.H. Lu, X.S. Chen, Z.G. Xie, T.C. Lu, X. Wang, J. Ma, X.B. Jing, Biomacromolecules 7 (2006) 1806–1810.
[38] L.C. You, F.Z. Lu, Z.C. Li, W. Zhang, F.M. Li, Macromolecules 36 (2003) 1–4.
[39] M. Toyoshima, Y. Miura, J. Polym. Sci.: Part A: Polym. Chem. 5 (2009) 1412–1421.